

## 2-d ESR diffusion coefficient imaging with the projection reconstruction method

T. Wokrina and E. Dormann\*

*Physikalisches Institut, Universität Karlsruhe (TH), D-76128 Karlsruhe, Germany*

Received 29 September 2003; revised 3 December 2003

### Abstract

The static gradient spin echo (SGSE) of the conduction electron spins in a quasi-one dimensional organic conductor is analyzed by simulation and for a microstructured (fluoranthene)<sub>2</sub>PF<sub>6</sub> single crystal. It is shown that useful two-dimensional magnetic resonance images of the diffusion coefficient (mobility)  $D$  can be obtained from pixel-by-pixel analysis of the signal decay with pulse separation  $\tau$ , adopting the projection reconstruction (PR) method for signal generation.

© 2003 Elsevier Inc. All rights reserved.

*Keywords:* Pulsed ESR; SGSE; Projection reconstruction; Quasi-one dimensional conductors; Conduction electron diffusion coefficient

### 1. Introduction

Non-destructive techniques of imaging sample properties are indispensable in materials science today. Magnetic resonance imaging (MRI) plays a very important role in this respect [1]. The favoured probes are the nuclear spins of the samples studied. They are spatially localized or only slowly moving, their relaxation times are long enough in order to allow pulsed gradient spin echo (PGSE) methods, and the isotopic variation of the gyromagnetic ratios allows to distinguish reliably between MRI of different elements or isotopes.

For the study of electronic properties of materials, MRI of the electron spins has to be applied [2]. Higher frequency ranges are accessible this way, but short transverse relaxation times of  $T_2 < 10 \mu\text{s}$  restricted PGSE techniques and Fourier imaging to some rare exceptions up to now [3–6]. Thus, the static gradient spin echo (SGSE) ESR-imaging offers clear advantages: The projection reconstruction (PR) with the Hahn echo (pulse separation time  $\tau$ ) is an easy implementable and controllable technique because no fast switching of gradients is necessary. However, it is not a priori clear that SGSE-PR-MRI can be applied at all to conduction

electron spins. It is not evident that it allows spatial resolution of dynamic properties. On the other hand, the application of spin echo-MRI is required for the analysis of typical organic conductors like the fluoranthene radical cation salts, as contrasted to CW-MRI, because the variation of the transversal relaxation time  $T_2$  (and correspondingly the CW-ESR linewidth) by a factor of two and more was discovered within one and the same crystal of such conductors [5]. Thus, the spatial  $T_2$ -variation has to be considered, even if only spin density imaging is attempted.

Here we focus on electron spin diffusion imaging that is of main interest for samples with spatially varying and anisotropic conduction electron mobility, like the quasi-one dimensional organic conductors [7–9]. Their diffusion coefficient  $D$  is larger by a factor of more than 1000 for motion of the conduction electron spins parallel to, as opposed to perpendicular to, the stacks of the organic radical cations. In addition, sample to sample variation of  $D$  by a factor of 50 was reported [9], and spatial variation of  $D$  by more than one order of magnitude was achieved in the same crystal by proton radiation damage [8]. We prove by simulation in comparison with an earlier “ad hoc” experiment of a microstructured single crystal [8] that reasonable two-dimensional (2-d) MRI of the diffusion coefficient  $D$  can indeed be obtained via SGSE-PR-MRI.

\* Corresponding author. Fax: +49-721-608-6103.

E-mail address: [edo@pi.uka.de](mailto:edo@pi.uka.de) (E. Dormann).

## 2. Principle of analysis

A 2-d spin density picture  $\tilde{\rho}(x, y, \tau)$  is constructed from measured projections  $S(\vec{k}, \tau)$  along directions  $\phi$  according to

$$\tilde{\rho}(x, y, \tau) = \int_0^{2\pi} d\phi \int_{-\infty}^{+\infty} dk S(\vec{k}, \tau) \cdot \exp[-2\pi i \vec{k} \cdot \vec{r}] \quad (1)$$

with

$$\vec{k} = (2\pi)^{-1} \gamma_e \vec{G} t \quad (2)$$

and

$$\phi = \tan^{-1}(G_y/G_x), \quad (3)$$

where  $\vec{G}$  is the magnetic field gradient and  $\gamma_e$  the gyromagnetic ratio of the conduction electron spin. This method has an inherent constraint concerning imaging anisotropic entities sensitive to changes of the gradient direction: During the measurement the sample properties and thus the projections may be altered and artefacts will be introduced into the image. This is in particular the case when imaging conduction electron spin diffusion in quasi-one dimensional organic conductors. We prove below by simulation in comparison with experiments in a microstructured (fluoranthene)<sub>2</sub>PF<sub>6</sub> single crystal that the artefacts can be reduced to a tolerable minimum. The spin dynamics are obtained by fitting to the explicit time dependence of each pixel  $\tilde{\rho}_{ij}$  the relation

$$\frac{\tilde{\rho}_{ij}(2\tau)}{\rho_{ij}(0)} = (1 - a) \cdot \exp\left(-\frac{2\tau}{T_{2,\text{del}}} - \frac{2}{3}\gamma^2 G^2 D \tau^3\right) + a \cdot \exp\left(-\frac{2\tau}{T_{2,\text{loc}}}\right) \quad (4)$$

In Eq. (4) a portion “*a*” of localized spins with possibly different relaxation time  $T_{2,\text{loc}}$  is considered in addition to the free spins with diffusion coefficient  $D$  and relaxation time  $T_{2,\text{del}}$  (portion  $(1 - a)$ ). In this manner, a 2-d map of diffusion coefficient  $D$ , portion “*a*,”  $T_{2,\text{loc}}$  or  $T_{2,\text{del}}$  can be obtained. This diffusion coefficient  $D$  is only an orientational average of the anisotropic properties of the organic conductor, however, by definition.

### 2.1. Simulation

The simulation models the diffusional process via the random walk. The jump distance  $\Delta r$  of a spin in one time step  $\Delta t$  is assumed to be Gauss-distributed (variable range hopping) so that  $(\Delta r^2)^{1/2} = (2D\Delta t)^{1/2}$  which is always chosen much smaller than all relevant length scales of the problem. This means that in this regime the diffusion is quasi-free. The resulting transient signal is then calculated by summing up all accumulated phase shifts due to the diffusional motion along the gradient.

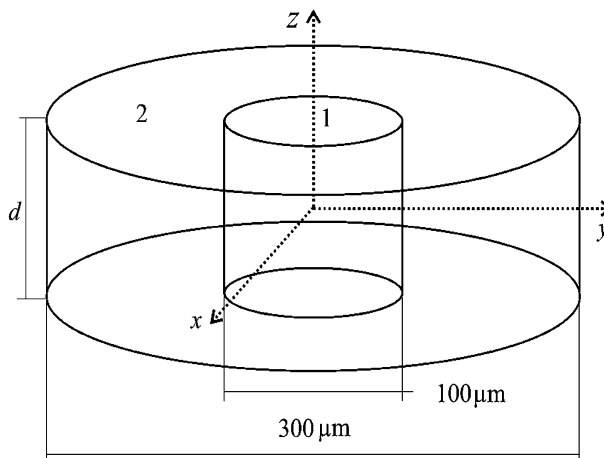


Fig. 1. Sample geometry used for numerical simulation.

Pore boundaries are assumed to be impermeable and perfectly reflecting. This allows for coherent back scattering of the spins so that the gradient of the magnetization normal to the pore surface vanishes. And also, relaxation on the pore surfaces is neglected.

The chosen sample geometry, two concentric cylinders “1” and “2,” is shown in Fig. 1. The inner part, pore “1,” is assumed highly anisotropic, with diffusion coefficient  $D_x = 0.2 \text{ cm}^2 \text{ s}^{-1}$  and  $D_x/D_y = 1000$ , typical for a fluoranthene radical cation salt [9], and  $T_2 = 6 \mu\text{s}$ . For the outer part, pore “2,” the same  $T_2$ -value, but isotropic diffusion,  $D_x/D_y = 1$ , is assumed. Thus, pore “2” presents the reference area where PR-imaging is known to operate [1]. The spin density is assumed to be constant within the sample (pores “1” and “2”) and zero outside. A typical ESR-MRI gradient of  $G = 0.8 \text{ Tm}^{-1}$  is used.

All projections in the  $x$ - $y$  plane were calculated as a function of the pulse separation  $\tau$  of the Hahn echo. The values of  $\tau$  were varied from 0.2 to 8  $\mu\text{s}$  in 0.1  $\mu\text{s}$  steps. Reconstructions of the spin density according to Eq. (1) are shown in Fig. 2 for three different  $\tau$  values. The 2-d spatially resolved map of the diffusion coefficient  $D$  and of the portion of localized spins “*a*” was then obtained by fitting the  $\tau$  dependence of the individual pixel  $(i, j)$  with Eq. (4) for  $\tau$  varying from 0.2 to 8  $\mu\text{s}$ . This result is shown in Fig. 3.

### 2.2. Experimental

Results for a “real” crystal of a quasi-one dimensional organic conductor, the arene radical cation salt (fluoranthene)<sub>2</sub>PF<sub>6</sub> have been reported recently [8]. They were based on a tentative (“ad hoc”) application of the SGSE-PR-MRI method. Fig. 4 shows this example for the spatial variation of the diffusion coefficient  $D$  in a microstructured crystal, derived with help of Eq. (4).

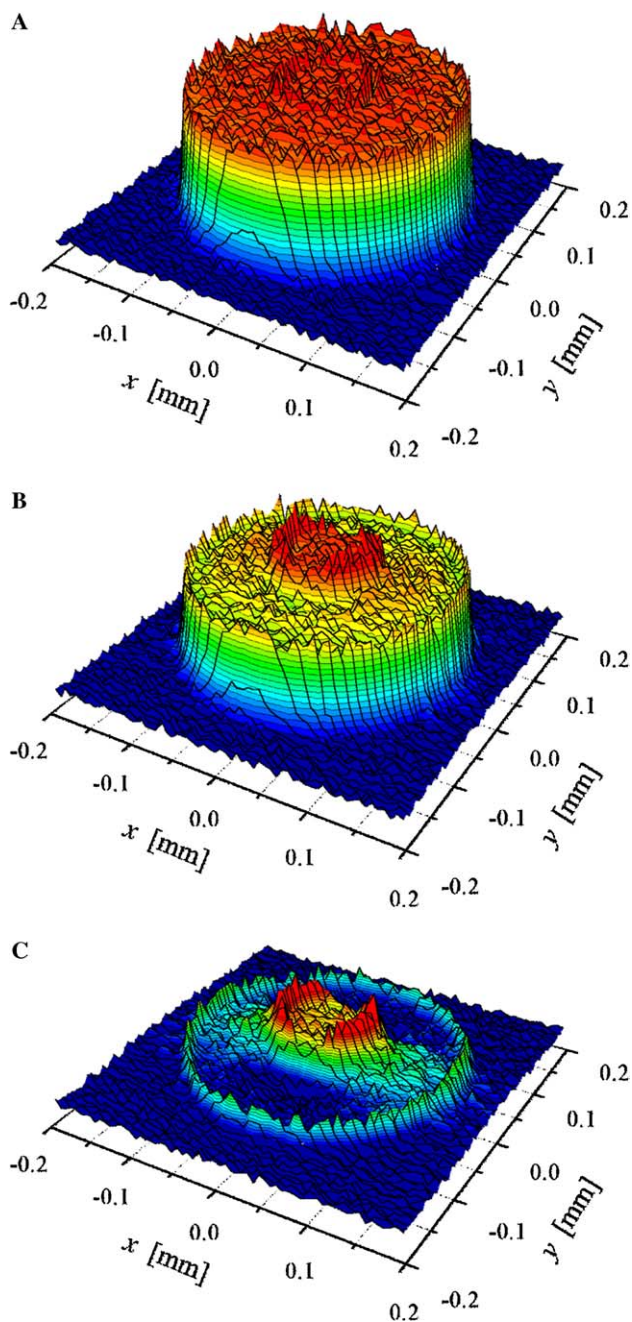


Fig. 2. 2-d reconstruction of  $\bar{\rho}$  as a function of  $\tau$  (simulation, geometry see Fig. 1). (A)  $\tau = 0.2 \mu\text{s}$ , (B)  $\tau = 1.0 \mu\text{s}$ , and (C)  $\tau = 2.0 \mu\text{s}$ .  $G = 0.8 \text{ Tm}^{-1}$ , resolution  $(8 \mu\text{m})^2$ .

The  $S(\vec{k}, \tau)$  data set was derived at X-band (9.5 GHz) with a Bruker ELEXSYS ESP E580 spectrometer. The static gradient of  $G = 0.81 \text{ Tm}^{-1}$  was realized with iron wedges on the pole caps of the electromagnet [8,9]. In order to be sensitive to imaging artefacts, a crystal was analyzed, whose properties were microstructured via proton irradiation through a slit mask with  $100 \mu\text{m}$  spacing of free and blocked areas. Evidently the induced 1-d spatial variation of the conduction electron diffusion coefficient is well resolved in the 2-d map of Fig. 4.

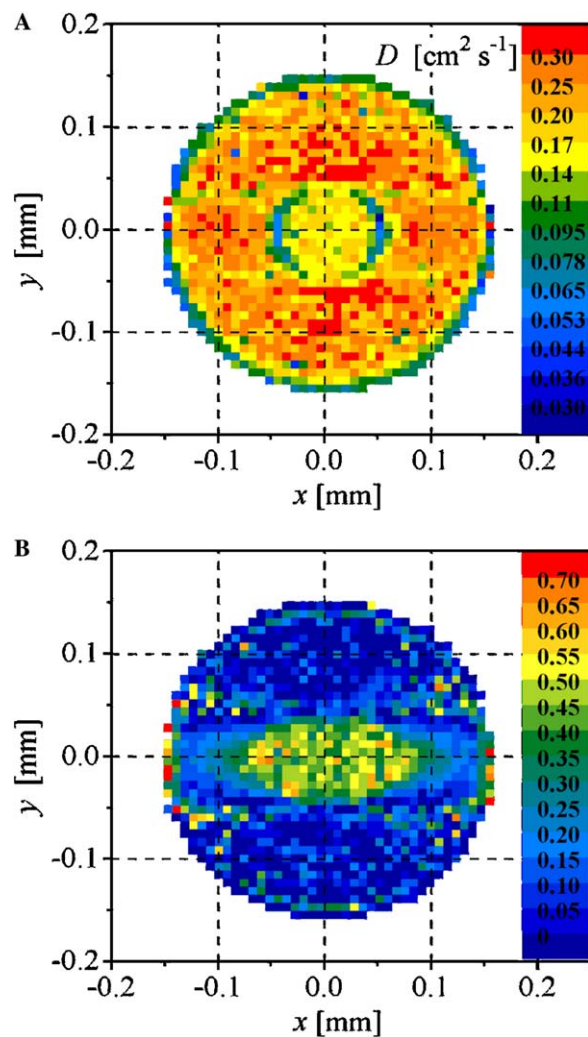


Fig. 3. 2-d spatially resolved map of the diffusion coefficient  $D$  and of the portion of localized spins “a” obtained by fitting Eq. (4) to the results of the numerical simulation (as shown in Fig. 2). Resolution  $(8 \mu\text{m})^2$ . (colored;  $D$ :  $0.03 \dots 0.3 \text{ cm}^2 \text{ s}^{-1}$ ; a:  $0 \dots 0.7$ ).

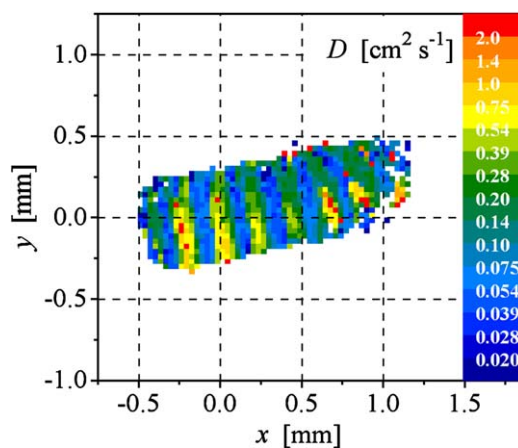


Fig. 4. 2-d spatially resolved map of the conduction electron diffusion coefficient  $D$  of a microstructured single crystal of the organic conductor (fluoranthene) $_2\text{PF}_6$  [8]. Pixel size  $(32 \mu\text{m})^2$  (unresolved third length  $550 \mu\text{m}$ ). (colored;  $D$ :  $0.02 \dots 2.0 \text{ cm}^2 \text{ s}^{-1}$ ).

### 3. Discussion

The reconstruction of  $\tilde{\rho}(x, y)$  as a function of  $\tau$  obtained from the random walk simulation shows that for very short times  $\tau$  (Fig. 2A) the image is not yet influenced by relaxation or diffusion and reflects the assumed homogeneous spin density. Only little noise is introduced by the statistical character of the random walk. As  $\tau$  becomes larger, the signal intensity decays. This happens because the spins lose their phase coherence. For the simulation, a rather large gradient was chosen so that this effect is dominated by diffusion and not by relaxation. It can already be seen in Fig. 2B that the signal is larger in pore “1,” because spin-motion is quasi-one dimensionally restricted there. At even longer times ( $\tau = 2\mu\text{s}$ , Fig. 2C) signal intensity decays very quickly except in regions near edges where diffusion is effectively restricted and thus coherence is conserved longer. This effect is often referred to as “edge enhancement” [1]. At  $\tau = 2\mu\text{s}$ , PR-MRI artefacts are evident in Fig. 2C: Signal intensity of pore “1” is beginning to “leak-out” along the  $x$ -axis, in spite of the impermeable walls assumed in the simulation. This is no surprise, because for the diffusion coefficient  $D_x = 0.2\text{ cm}^2\text{ s}^{-1}$ , the conduction electron spin reaches a root mean square averaged displacement  $\langle\delta r_x\rangle = (\delta r_x^2)^{1/2} = (2D_x \cdot 2\tau)^{1/2} = 12.6\mu\text{m}$  at the time of the SGSE for  $\tau = 2\mu\text{s}$ , the longest pulse separation used in the simulations of Fig. 2, thus comparable to the resolution of  $8\mu\text{m}$  adopted. For the perpendicular direction  $\langle\delta r_y\rangle = 0.4\mu\text{m}$  is still negligible for  $D_x/D_y = 1000$  under these conditions. Therefore the projections recorded with field gradient along the  $y$  direction are attenuated much less in pore “1” than in pore “2” (shell). This evidently gives rise to this observed PR-imaging artefact.

Fig. 3A shows one result of the fit of Eq. (4) to the random walk simulation data—the 2-d spatially resolved map of the diffusion coefficient  $D$ . Qualitatively the major features are displayed correctly. Quantitatively, in the uniform pore “2”  $D$  is overestimated by approximately 50% whereas in pore “1,” where  $D_y = D_x/1000$  was assumed, the numerical analysis reflects the value of  $D_x$  with good precision instead of the correct average value  $D = (D_x + D_y)/2 \approx D_x/2$ . At all edges the motion is spatially restricted. Consequently  $D$  is reduced by up to one order of magnitude. Only little distortions along the  $x$ -axis can be seen in the  $D(x, y)$  map. It should be stressed, however, that all signs of the anisotropy of the diffusion coefficient  $D$  are lost. For the anisotropy used in the simulations, i.e.,  $D_x/D_y = 1000$ , the much larger value of  $D_x$  dominates the  $D(x, y)$  map. The reanalysis of the 2-d reconstruction of  $\tilde{\rho}(x, y, \tau)$  with Eq. (4) indicated larger artefacts for the portion of localized spins, “ $a$ ” (Fig. 3B). For “ $a$ ,” the cylindrical symmetry of the simulation model

assumption, i.e., “ $a$ ” = 0, is lost. Thus the portion of localized spins seems to take care of the PR-imaging artefacts here.

These findings are supported by our earlier “ad hoc” SGSE-PR-MRI of the conduction electron spins of the quasi-one dimensional organic conductor (fluoranthene)<sub>2</sub>PF<sub>6</sub> [8]. For very small gradient  $G$  the conditions for the PR-MRI are not questioned and 2-d maps of the transversal relaxation times could be derived [8], in reasonable agreement with the results of Fourier imaging with the PGSE technique [5]. The results for the conduction electron diffusion coefficient presented in Fig. 4 for a microstructured (proton irradiation damaged) crystal are self explanatory. Here the irradiated regions exhibit a  $D$  value reduced approximately by a factor of 30 compared to regions protected by the slit mask. The geometry corresponds nicely to the one of the mask and only little distortions are experienced. Again, however, the portion of localized spins derived from fitting Eq. (4) to the individual pixel  $\rho_{ij}(2\tau)$  variation seemed to suffer more from imaging artefacts. By comparing the metrics and the  $D_{\parallel}$  values derived independently from a 1-d projection, no significant differences could be discerned. Thus we may conclude that the 2-d diffusion map accessible by SGSE-PR-MRI using fitting of the individual pixel signal  $\tilde{\rho}_{ij}(2\tau)$  with Eq. (4) (see Figs. 3 and 4 for examples) constitutes a reliable representation of  $D_{\parallel}(x, y)$ .

### 4. Concluding remarks

A priori it is not clear that static gradient spin echo projection reconstruction magnetic resonance imaging (SGSE-PR-MRI) can be used in presence of anisotropic properties, sensitive to the gradient direction, like highly anisotropic conduction electron spin diffusion in quasi-one dimensional organic conductors. With help of numerical simulations and measurements of the quasi-one dimensional organic conductor (fluoranthene)<sub>2</sub>PF<sub>6</sub> it could be verified, however, that a reasonable, high resolution 2-d spatial mapping of diffusion properties can be obtained in spite of inherent systematic errors by using the PR procedure. No evidence is given about the anisotropy of the diffusion coefficient, however, and the portion of localized spins distributed on crystal surfaces or interior boundaries seems to suffer more severely under imaging artefacts.

### Acknowledgments

We thank G. Alexandrowicz, A. Feintuch, and N. Kaplan for discussions, and the Deutsche Forschungsgemeinschaft for financial support (Grant Do 181/10).

**References**

- [1] P.T. Callaghan, *Principles of Nuclear Magnetic Resonance Microscopy*, Oxford University Press, Oxford/New York, 1991.
- [2] S.S. Eaton, G.R. Eaton, in: M.J. Davis, B.C. Gilbert, K.A. McLauchlan (Eds.), *EPR*, vol. 17, 2000, p. 109.
- [3] T. Tashma, G. Alexandrowicz, N. Kaplan, E. Dormann, A. Grayevsky, A. Gabay, *Synth. Metals* 106 (1999) 151.
- [4] G. Alexandrowicz, T. Tashma, A. Feintuch, A. Grayevsky, E. Dormann, N. Kaplan, *Phys. Rev. Lett.* 84 (2000) 2973.
- [5] T. Tashma, A. Feintuch, A. Grayevsky, J. Gmeiner, A. Gabay, E. Dormann, N. Kaplan, *Synth. Metals* 132 (2003) 161.
- [6] A. Feintuch, T. Tashma, A. Grayevsky, J. Gmeiner, E. Dormann, N. Kaplan, *J. Magn. Res.* 157 (2002) 69.
- [7] E. Dormann, *Physikal. Blätter* 39 (1983) 221.
- [8] T. Wokrina, J. Gmeiner, N. Kaplan, E. Dormann, *Phys. Rev. B* 67 (2003) 054103.
- [9] T. Wokrina, J. Gmeiner, N. Kaplan, E. Dormann, *Eur. Phys. J. B* 35 (2003) 191.